Apolar *ortho*-phenylene ethynylene oligomers: conformational ordering without intermolecular aggregation†

Jing Jiang, Morris M. Slutsky, Ticora V. Jones and Gregory N. Tew*

Received (in Gainesville, FL, USA) 19th May 2009, Accepted 27th September 2009
First published as an Advance Article on the web 24th November 2009
DOI: 10.1039/b9nj00200f

This paper describes the characterization of solvent induced folding behavior for non-polar (NP) alkoxy substituted *ortho*-phenylene ethynylene (*o*-PE) oligomers. Oligomers of lengths up to nine units have been shown to adopt helical conformations in heptane by NMR and CD spectroscopy, while chloroform promotes extended conformations. Surprisingly, the molar ellipticity values found in heptane for these oligomers are very small compared to other literature values of *meta*-phenylene ethynylene (*m*-PE) folded systems; however, comparable molar ellipticity values were found for a closed macrocyclic *o*-PE suggesting the weak ellipticity is a molecular-feature rather than a quality of folding indicator.

Introduction

Foldamers[1] continue to attract interest in various fields such as biomimetics, catalysis, supramolecular assembly, *etc*.[2–8] Among the various types of foldamers, one class is based on aromatic molecules including those with the phenylene ethynylene backbone.[9] Solvent has been routinely used in the study of aromatic systems to induce or disrupt folding. Taking advantage of the contrast between the side chain and the backbone, it has been shown that a good solvent for the side chain which is also a bad solvent for the backbone drives folding. This has been referred to as solvophobic induced folding. When a molecule with a polar side chain and an apolar backbone is introduced to a polar medium, the molecular heterogeneity of the structure is segregated such that a secondary structure, a helix of *ortho*- or *meta*-phenylene ethynylene oligomers, is formed.[10,11] This helix allows the non-polar (NP) backbone to collapse, reducing its interaction with the solvent, while the polar side chains are favorably solvated.

Previously, we reported the synthesis of short *ortho*-phenylene ethynylene (*o*-PE) oligomers containing polar triethylene glycol monomethyl ether (Teg) side groups. 1D and 2D solution NMR spectroscopy clearly showed evidence of helical folding in these oligomers.[11] However, the folding behavior of NP substituted *o*-PE oligomers has not yet been reported. In this paper, a series of *o*-PE oligomers (**1–4**) with lengths of up to nine units substituted with chiral alkoxy side chains are studied by NMR, UV and circular dichroism (CD) spectroscopy. UV and CD have been commonly used by Moore *et al*. in their studies of the *meta*-phenylene ethynylene (*m*-PE) system.[10,12]

Department of Polymer Science and Engineering, University of Massachusetts, Amherst, MA 01003, USA. E-mail: tew@mail.pse.umass.edu; Fax: +1 413 545 0082; Tel: +1 413 577 1612

† Electronic supplementary information (ESI) available: Detailed procedures and additional characterization of monomers and dimers. See DOI: 10.1039/b9nj00200f

Results and discussion

The NP *o*-PE oligomers were synthesized following previously reported procedures (ESI†).[11] Fig. 1 shows the chemical structure of nonamer **4** to highlight the side chains and molecular backbone. The introduction of NP side chains allows us to explore whether the contrast between the alkyl side chains and the highly conjugated apolar backbone produces enough heterogeneity in the molecule to allow solvophobically induced helix formation in alkane based solvents. As shown in Fig. 1, our NP side chain is based on (−)-*S*-methylbutane while many of the other molecules in the literature have used longer side chains (typically greater than 9 carbons) to induce contrast.[13–16]

It has been shown previously through extensive NMR studies that Teg substituted versions of these *o*-PE oligomers take on compact helical structures. Detailed 1D and 2D NMR analysis provided clear evidence of upfield shifts due to the π–π stacking for only the signals corresponding to those aromatic protons involved in folding. NOESY/ROESY 2D NMR data also exhibited cross peaks between the terminal TMS and aromatic or triazene protons on the oligomers that are only possible if the *o*-PE is in a compact helical conformation.

In accordance with these previous studies, ^{1}H NMR spectroscopy proves to be an indispensable tool for the oligomers

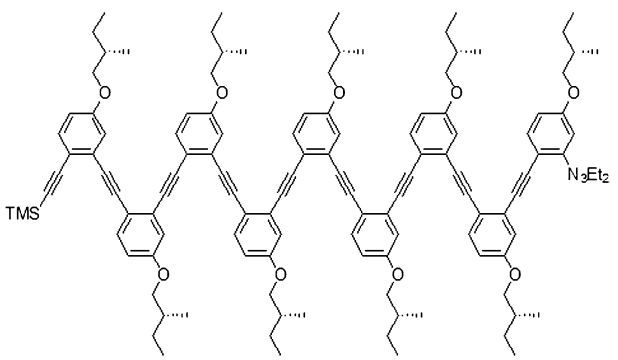

Fig. 1 Structure of alkoxy substituted nonamer **4**.

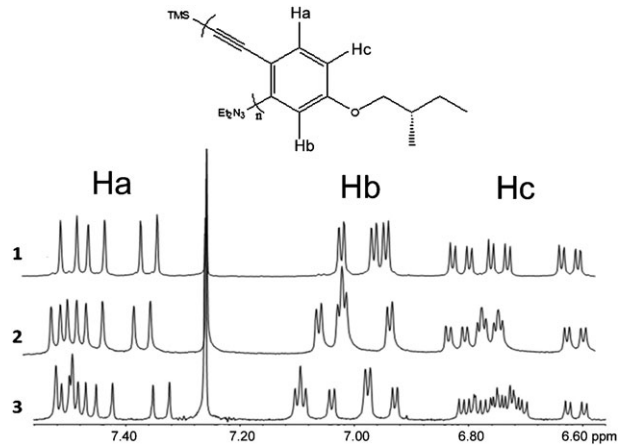

Fig. 2 Expansions of the aromatic regions of the ^{1}H NMR spectra for trimer **1** (n = 3), tetramer **2** (n = 4), and hexamer **3** (n = 6) in $CDCl_3$. Each ring has three protons that are labeled respective to their J-coupling and splitting pattern: Ha (8.4 Hz, d); Hb (2.1 Hz, d); and Hc (8.4 Hz and 2.1 Hz, dd).

described here. Fig. 2 shows the abbreviated structure for the *o*-PE oligomers and the aromatic regions of trimer **1**, tetramer **2**, and hexamer **3** in $CDCl_3$ at 400 MHz. Each unique aromatic peak lies within the areas labeled as Ha, Hb and Hc. Dispersion is exhibited in the aromatic regions as all 9, 12, and 18 protons can be counted and assigned to specific ring systems by J-coupled correlation spectroscopy (COSY).[11c]

To determine whether an alkane based solvent would have an impact on the upfield shifting and therefore the π–π stacking in the aromatic region of these NP *o*-PEs, deuterated heptane (d_{16}-hept) was used as the folding solvent. Fig. 3(a) shows the aromatic region of tetramer **2** in d_{16}-hept (top) and in $CDCl_3$ (bottom). Protons on rings 1 and 4 of this oligomeric system are labeled. There are clear upfield shifts for protons Ha1 and Ha4 as well as Hc1 and Hc4, when the solvent changes from chloroform to heptane. This is exactly consistent with the upfield shifts observed in our previous report, which were caused by the π–π stacking of rings 1 and 4 (see Fig. 3(b)), and confirmed by 2D NOESY studies.[11] Fig. 3(a) shows that proton Hb1 shifts upfield while proton Hb4 shifts downfield slightly. Although the exact origins of these shifts are not completely understood, based on the molecular model shown in Fig. 3(b), Hb1 should shift upfield as it resides over the triple bond while Hb4 might shift downfield since it is located under the non-aromatic TMS group.

The ^{1}H NMR data in Fig. 4 for nonamer **4** were taken at 600 MHz in d_{16}-hept (top) and $CDCl_3$ (bottom). Though particular assignments are difficult to make, a clear difference is seen in the aromatic regions between d-heptane and $CDCl_3$ and it appears that *all* of the aromatic peaks shift *upfield* in the folding solvent (d_{16}-hept), consistent with the expectation of a fully folded structure. There is still excellent dispersion thus large and uncontrolled aggregation can be ruled out even at longer lengths of this *o*-PE system. While some of the Ha peaks in the $CDCl_3$ spectra are obscured by the solvent, it is clear that all 9 Hb and Hc peaks are present and shift upfield accordingly, which provides strong support for helix formation in these NP *o*-PE oligomers.[17]

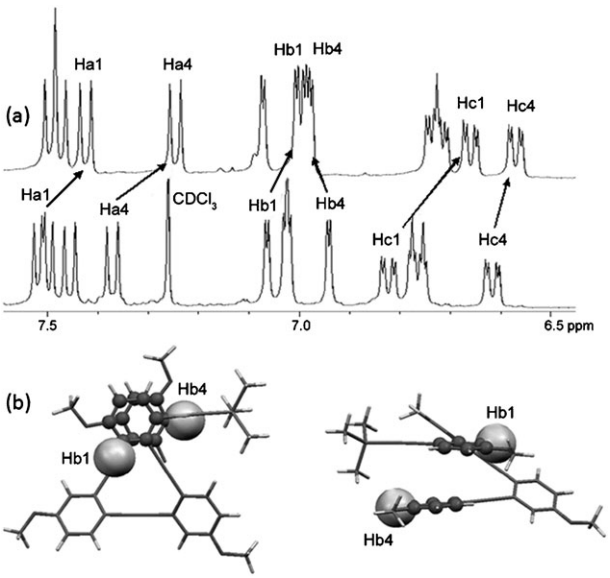

Fig. 3 (a) The aromatic region in ^{1}H NMR spectra of tetramer **2** in d_{16}-heptane (top) and $CDCl_3$ (bottom). (b) Molecular model of tetramer **2**, top and side view.

Unfortunately, no NOE cross peaks are observed in these systems due to the strong d_{16}-hept solvent peak. Nevertheless, we have previously documented the relationship between through-space NOE signals and 1D upfield NMR shifts in these *o*-PE folded structures. Therefore, the 1D NMR spectra shown in Fig. 3(a) and 4 are completely consistent with folded helical structures.

UV proved to be a useful tool for distinguishing folded and unfolded states in *m*-PE oligomers.[10,12] Six-unit macrocycles were used to confirm the absorption bands assigned to the cisoid conformations required in the folded structure. The difference between transoid and cisoid conformations was observed with changing solvent for the *m*-PE systems. Unfortunately the same comparison cannot be made for *o*-PE systems. Fig. 5(a–c) shows UV spectra for oligomers **1–4** in chloroform (a), heptane (b), and a comparison of nonamer **4** with macrocycle **5** (c). There is little to no relationship between the macrocycle and the *o*-PE oligomers as peaks at

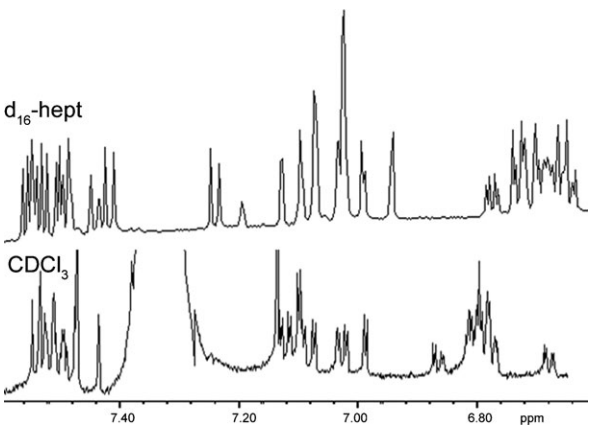

Fig. 4 ^{1}H NMR traces of the aromatic region of nonamer **4** in d_{16}-heptane (top) and $CDCl_3$ (bottom).

285 and 315 nm in the macrocycle do not correlate well with the peaks at 275 and 350 nm in the *o*-PE oligomers. This difference is likely explained by the *ortho*-connection in this PE macrocycle. The changes in UV profile in solvent for oligomers **1–4** are extremely subtle and do not provide robust data for clear interpretation, in sharp contrast to the *m*-PE systems.

Unlike the UV results, CD provides an additional mechanism for probing helicity of the NP *o*-PE oligomers, given the chiral nature of the alkoxy side chain. CD has been used as a method to examine secondary structures of biological macromolecules and foldameric systems.[18–21] Fig. 6(a) shows the CD spectra of nonamer **4** in chloroform (0.268 mM) at 0 °C as well as in *n*-heptane (0.167 mM) at 0, 10, and 20 °C. The purpose of these experiments was to determine whether a helical conformation is obtained in *n*-heptane *versus* an extended conformation in chloroform. In addition, a decrease in temperature should favor a folded structure. There is little to no ellipticity for the nonamer in chloroform, even at 0 °C and higher concentration while there is a comparatively substantial signal for the nonamer in *n*-heptane even at room temperature although the ellipticity is strongest at 0 °C.

Additional CD data for oligomers **2–4** indicate that there is a slight length dependence for ellipticity in *n*-heptane while each oligomer exhibits a lack of coherent signal in chloroform at room temperature. This length dependence is reasonable as tetramer **2** would represent only one and one third turn of a helix while hexamer **3** and nonamer **4** represent two and three turns of the helix, respectively. A temperature study of hexamer **3** in heptane shows a stronger ellipticity with decreasing temperature much like the data shown in Fig. 6(a) for the nonamer. To determine whether concentration has an impact on the obtained spectra, the concentration and path length were altered by an order of magnitude each (concentration increased, path length decreased) such that absorbance should remain constant. The lack of dramatic change in the resulting spectra leads to the conclusion that the data shown in Fig. 6(a) are the result of non-aggregated NP *o*-PE entities in the helical state, indicating a lack of large scale aggregation that could create an undefined but CD-active structure.

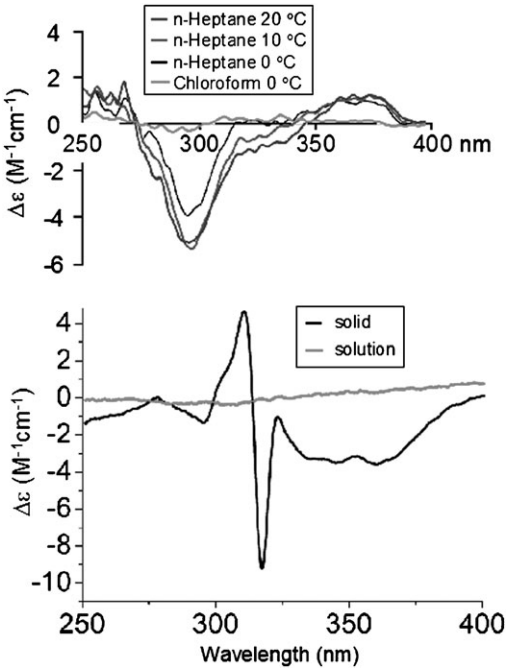

Fig. 6 (top) CD spectra of nonamer **4** in $CHCl_3$ (0.268 mM) and *n*-heptane at 0, 10 and 20 °C at 0.167 mM. (bottom) CD spectra traces of macrocycle **5** in solution and in the solid state on quartz.

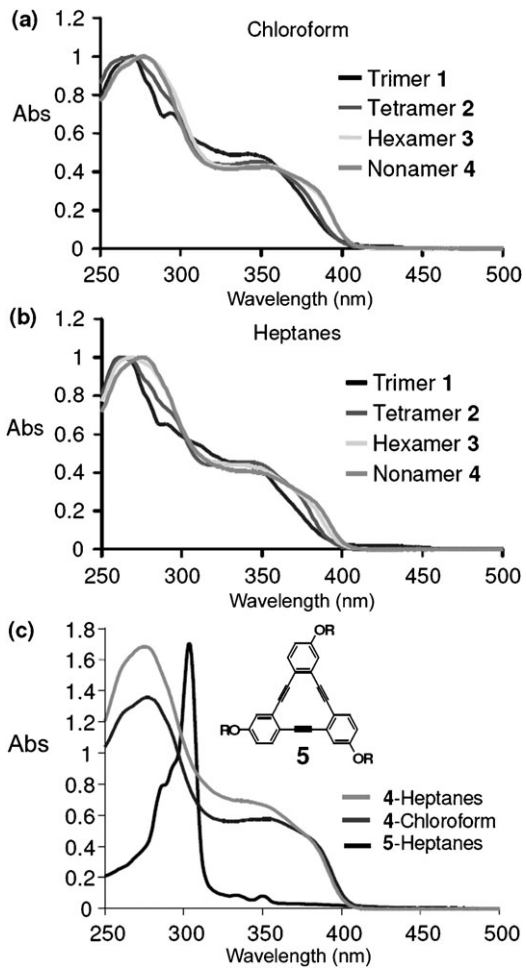

Fig. 5 UV-Vis spectra of oligomers **1–4** in chloroform (a), *n*-heptane (b) and a comparison of nonamer **4** with macrocycle **5** (c) (structure shown in inset) at 12.5 μM.

While these data are encouraging, the molar ellipticity ($\Delta\varepsilon$) values are significantly less than what has been reported for other synthetic macromolecular and biological systems in the literature.[10,22,23] In particular, the system most closely related to these, the apolar *m*-PE foldamer exhibits ellipticity values between −300 and 300 (M^{-1} cm^{-1}) for an oligomer with 3 helical turns.[22,23] Additionally, the CD signals derived from those NP *m*-PE systems appear to be time and temperature dependent, showing signs of intermolecular aggregation. To further understand the CD behavior of these *o*-PE oligomers, the CD spectrum of a model macrocycle was studied in the solid state (see Fig. 6(b)) where this molecule is known to form a highly ordered liquid crystal.[24] The observed CD signals of this ordered system show similarly small $\Delta\varepsilon$ values compared to the solutions of folded nonamer **4** in Fig. 6(a).

The CD signal intensity can be affected by various parameters.[25] Meijer *et al*. reported that the location of the chiral center with relation to the chromophore greatly impacts the resulting CD spectra.[20] The angle of exciton coupled transition moments has a large impact on the observed CD intensity with a maximum observed at 70° which decays to null at zero degrees.[25e] Naphthalene–diimide systems studied by Matile *et al*. illustrate this nicely.[25a,b] Additionally, the intensity decreases with increasing distance between the chromophores and is proportional to the extinction coefficient.[25e] The pitch of the helical twist can also impact the CD intensity. As a result of these variables, the strict assignment of CD intensity to helical content can be misleading. The small molar ellipticity values of the ordered macrocycle lead to the conclusion that these *o*-PE systems have inherently small CD signals.

Experimental

General

All solvents were purified through a standard protocol. All commercial chemicals were used without further purification. ^{1}H NMR spectra were obtained from a Bruker DPX 400 MHz spectrometer or 600 MHz spectrometer by means of a TXI probe with Z-gradient capabilities. The temperature was maintained at 305 K for all acquisitions. UV-visible spectra were recorded on a Hewlett-Packard 8453. CD spectra were taken on a JASCO J720 spectrometer in rectangular cuvettes. The procedure for all monomers and dimer is shown in the ESI†.

General TMS deprotection procedure

One equivalent of the TMS protected compound and 2.5 molar equivalents of K_2CO_3 with 5–10 mL of methanol (and 5–10 mL THF if necessary for solubility) were stirred in a nitrogen-flushed vial for 0.5 to 3 h. The reaction was monitored by TLC. Upon completion, the solution was diluted with ethyl acetate and water and washed twice with water. After drying the ethyl acetate layer over $MgSO_4$ and evaporation of solvent, the residue was purified by flash chromatography.

General triazene activation procedure

A Schlenk flask with a stir bar was flame dried under vacuum and backfilled with N_2 three times. The triazene compound was dissolved in enough distilled methyl iodide to make a 0.1 M solution and transferred to the Schlenk flask. The Schlenk flask was then gently degassed for 30 s then backfilled with N_2 and closed. The reaction vessel was placed in a 110 °C oil bath for 6–18 h, and monitored by TLC. Upon completion, the reaction mixture was diluted with hexanes, filtered over Celite, concentrated and purified by flash chromatography.

General Sonogashira coupling procedure

A Schlenk flask with a stir bar was flame dried under vacuum and backfilled with N_2 three times. To this flask were added 0.05–0.1 equivalents (based on the acetylene compound) of $Pd(PPh_3)_2Cl_2$ and 0.1–0.2 equivalents of CuI. The 1–1.1 equivalents of the acetylene compound to 1 equivalent iodide compound were dissolved in separate flasks in triethylamine (TEA) and transferred *via* syringe to the Schlenk flask under N_2. The Schlenk flask was gently degassed for 30 s then backfilled with N_2. The flask was sealed and placed in an oil bath at 45 °C for 6–18 h and checked by TLC for completeness. Once done, the reaction solution was diluted with ether, filtered through a pad of Celite and concentrated. The residue was then purified by flash chromatography.

Trimer 1

Trimer **1** was synthesized from TMS deprotected dimer (**D-H**) and **M5** (ESI†) following the general Sonogashira coupling procedure with yield of 60%. ^{1}H NMR ($CDCl_3$, ppm) δ: 7.45 (1H, d, J = 8.53 Hz), 7.44 (1H, d, J = 8.62 Hz), 7.35 (1H, d, J = 8.63 Hz), 7.01 (1H, d, J = 2.57 Hz), 6.96 (1H, d, J = 2.60 Hz), 6.94 (1H, d, J = 2.51 Hz), 6.80 (1H, dd, J = 8.62, 2.60 Hz), 6.74 (1H, dd, J = 8.62, 2.60 Hz), 6.61 (1H, dd, J = 8.54, 2.56 Hz), 3.87–3.68 (8H, m), 3.63–3.50 (2H, m), 1.93–1.68 (4H, m), 1.63–1.37 (4H, m), 1.34–1.10 (12H, m), 1.04–0.84 (21H, m), 0.24 (9H, s). MS: m/z 732.

TMS deprotected trimer (1-H)

TMS deprotected trimer (**1-H**) was obtained from trimer **1** *via* the general TMS deprotection procedure in quantitative yield. ^{1}H NMR ($CDCl_3$, ppm) δ: 7.50 (1H, d, J = 8.69 Hz), 7.47 (1H, d, J = 8.85 Hz), 7.37 (1H, d, J = 8.61 Hz), 7.02 (1H, d, J = 2.59 Hz), 6.99 (1H, d, J = 2.62 Hz), 6.95 (1H, d, J = 2.55 Hz), 6.80 (1H, dd, J = 8.61 Hz, 2.62 Hz), 6.77 (1H, dd, J = 8.61 Hz, 2.64 Hz), 6.63 (1H, dd, J = 8.55 Hz, 2.56 Hz), 3.9–3.5 (10H, m), 3.16 (1H, s), 1.95–1.7 (3H, m), 1.65–1.4 (3H, m), 1.36–1.08 (9H, m), 1.01 (3H, d, J = 6.74 Hz), 1.00 (3H, d, J = 6.73 Hz), 0.94 (3H, d, J = 6.74 Hz), 0.94 (6H, t, J = 7.62 Hz), 0.89 (3H, t, J = 7.6 Hz).

Triazene activated trimer (1-I)

Triazene activated trimer (**1-I**) was obtained from trimer **1** *via* the general triazene activation procedure with a yield of 88%. ^{1}H NMR ($CDCl_3$, ppm) δ: 7.49 (2H, d, J = 8.62 Hz), 7.38 (1H, d, J = 8.62 Hz), 7.37 (1H, d, J = 2.47 Hz), 7.10 (1H, d, J = 2.46 Hz), 7.03 (1H, d, J = 2.51 Hz), 6.89–6.70 (3H, m), 3.90–3.59 (6H, m), 1.95–1.72 (3H, m), 1.66–1.42 (3H, m), 1.36–1.12 (3H, m), 1.07–0.84 (18H, m), 0.21 (9H, s).

Tetramer 2

Tetramer **2** was synthesized from TMS deprotected trimer (**1-H**) and **M5** (see ESI†) following the general Sonogashira coupling procedure with a yield of 45%. ^{1}H NMR ($CDCl_3$, ppm) δ: 7.51 (d, 1H, J = 8.72 Hz), 7.50 (d, 1H, J = 8.72 Hz), 7.45 (d, 1H, J = 8.44 Hz), 7.37 (d, 1H, J = 8.72 Hz), 7.06 (d, 1H, J = 2.73 Hz), 7.02 (d, 1H, J = 1.84 Hz), 7.01 (d, 1H, J = 2.73 Hz), 6.94 (d, 1H, J = 2.49 Hz), 6.82 (dd, 1H, J = 2.76 Hz, 8.56 Hz), 6.79–6.73 (m, 2H,), 6.61 (dd, 1H, J = 2.55 Hz, 8.56 Hz), 3.96–3.54 (m, 12H), 1.90–1.68 (m, 4H), 1.63–1.46 (m, 4H), 1.36–1.18 (m, 10H), 1.03–0.83 (m, 24H), 0.24 (s, 9H). MS: m/z 918.

Hexamer 3

Hexamer **3** was synthesized from TMS deprotected trimer (**1-H**) and triazene activated trimer (**1-I**) following the general Sonogashira coupling procedure with a yield of 52%. ^{1}H NMR ($CDCl_3$, ppm) δ: 7.53 (2H, d, J = 8.59 Hz), 7.52 (1H, d, J = 8.63 Hz), 7.50 (1H, d, J = 8.57 Hz), 7.46 (1H, d, J = 8.63 Hz), 7.36 (1H, d, J = 8.65 Hz), 7.12 (1H, d, J = 2.77 Hz), 7.11 (1H, d, J = 2.84 Hz), 7.06 (2H, d, J = 2.56 Hz), 6.99 (1H, d, J = 2.56 Hz), 6.95 (1H, d, J = 2.51 Hz), 6.84–6.72 (5 H, m), 6.63 (1H, dd, J = 8.65 Hz, 2.69 Hz), 3.89–3.52 (m, 16H), 1.97–1.68 (6H, m), 1.663–1.41 (8H, m), 1.39–1.08 (16H, m), 1.08–0.75 (40H, m), 0.26 (9H, s). MS m/z = 1290.

TMS deprotected hexamer (3-H)

TMS deprotected hexamer (**3-H**) was obtained from hexamer **3** through the general TMS deprotection procedure in quantitative yield. ^{1}H NMR ($CDCl_3$, ppm) δ: 7.50 (1H, d, J = 8.69 Hz), 7.47 (1H, d, J = 8.85 Hz), 7.37 (1H, d, J = 8.61 Hz), 7.02 (1H, d, J = 2.59 Hz), 6.99 (1H, d, J = 2.62 Hz), 6.95 (1H, d, J = 2.55 Hz), 6.80 (1H, dd, J = 8.61 Hz, 2.62 Hz), 6.77 (1H, dd, J = 8.61 Hz, 2.64 Hz), 6.63 (1H, dd, J = 8.55 Hz, 2.56 Hz), 3.9–3.5 (10H, m), 3.16 (1H, s), 1.95–1.70 (3H, m), 1.65–1.40 (3H, m), 1.36–1.08 (9H, m), 1.01 (3H, d, J = 6.74 Hz), 1.00 (3H, d, J = 6.73 Hz), 0.94 (3H, d, J = 6.74 Hz), 0.94 (6H, t, J = 7.60 Hz), 0.89 (3H, t, J = 7.60 Hz).

Nonamer 4

Nonamer **4** was synthesized from TMS deprotected hexamer (**3-H**) and triazene activated trimer (**1-I**) following the general Sonogashira coupling procedure with a yield of 49%. ^{1}H NMR ($CDCl_3$, ppm) δ: 7.53 (2H, d, J = 8.59 Hz), 7.52 (1H, d, J = 8.63 Hz), 7.50 (1H, d, J = 8.57 Hz), 7.46 (1H, d, J = 8.63 Hz), 7.36 (1H, d, J = 8.65 Hz), 7.12 (1H, d, J = 2.77 Hz), 7.11 (1H, d, J = 2.84 Hz), 7.06 (2H, d, J = 2.56 Hz), 6.99 (1H, d, J = 2.56 Hz), 6.95 (1H, d, J = 2.51 Hz), 6.84–6.72 (5H, m), 6.63 (1H, dd, J = 8.6, 2.6 Hz), 3.89–3.52 (m, 16H), 1.97–1.68 (6H, m), 1.66–1.41 (8H, m), 1.39–1.08 (16H, m), 1.07–0.74 (40H, m), 0.26 (9H, s). MS m/z = 1850.

Conclusions

A number of studies were performed to induce and observe a helical secondary structure for these alkoxy substituted NP *o*-PE oligomers. ^{1}H NMR experiments exhibited upfield shifts in the aromatic region indicating π–π stacking in d_{16}-heptane. All protons for nonamer **4** moved upfield while only protons associated with rings 1 and 4 in tetramer **2** moved upfield, consistent with helix formation. UV data proved too ambiguous to identify distinctive changes with increasing *o*-PE length in heptane as opposed to chloroform. A comparison of the three-unit macrocycle to the *o*-PE oligomer proved to be of little utility, as a correlation between the cisoid structure and a folding oligomer could not be found due to the *ortho*-connectivity of the macrocycle. CD spectra did exhibit elements of length, solvent, and temperature dependence for the resulting ellipticity values of these *o*-PE oligomers. These signals appeared to be strongest for nonamer **4** in *n*-heptane at 0 °C. Though these values were 2–3 orders of magnitude smaller than other reported literature values, similarly small values for the ordered macrocycle in the solid state were obtained, supporting helix formation.

Acknowledgements

We thank the NSF for financial support (NSF CAREER CHE-0449663). T.V.J. thanks the Ford Foundation for financial support. G.N.T thanks the ARO and ONR Young Investigator programs in addition to the PECASE program, 3M Nontenured faculty grant, and Dupont Young Faculty Award for generous support. Tatyana Shalapyonok is specially acknowledged for her contributions in the monomer synthesis.

Notes and references

1 S. H. Gellman, *Acc. Chem. Res.*, 1998, **31**, 173.
2 (*a*) R. P. Cheng, S. H. Gellman and W. F. Degrado, *Chem. Rev.*, 2001, **101**, 3219; (*b*) D. J. Hill, M. J. Mio, R. B. Price, T. S. Hughes and J. S. Moore, *Chem. Rev.*, 2001, **101**, 3893; (*c*) P. Cheng, *Curr. Opin. Struct. Biol.*, 2004, **14**, 512; (*d*) M. S. Cubberley and B. L. Iverson, *Curr. Opin. Chem. Biol.*, 2001, **5**(6), 650–653.
3 N. Zhu, W. Hu, S. Han, Q. Wang and D. Zhao, *Org. Lett.*, 2008, **10**, 4283.
4 W. S. Horne, M. D. Boersma, M. A. Windsor and S. H. Gellman, *Angew. Chem., Int. Ed.*, 2008, **47**, 2853.
5 C. Bao, B. Kauffmann, Q. Gan, K. Srinivas, H. Jiang and I. Huc, *Angew. Chem., Int. Ed.*, 2008, **47**, 4153.
6 R. M. Meudtner and S. Hecht, *Angew. Chem., Int. Ed.*, 2008, **47**, 4926.
7 V. Bradford and B. L. Iverson, *J. Am. Chem. Soc.*, 2008, **130**, 1517.
8 W. Cai, G. Wang, Y. Xu, X. Jiang and Z. Li, *J. Am. Chem. Soc.*, 2008, **130**, 6936.
9 R. A. Smaldone and J. S. Moore, *Chem.–Eur. J.*, 2008, **14**, 2650.
10 (*a*) J. C. Nelson, J. G. Saven, J. S. Moore and P. G. Wolynes, *Science*, 1997, **277**, 1793; (*b*) R. B. Prince, J. G. Saven, P. G. Wolynes and J. S. Moore, *J. Am. Chem. Soc.*, 1999, **121**, 3114; (*c*) D. J. Hill and J. S. Moore, *Proc. Natl. Acad. Sci. U. S. A.*, 2002, **99**, 5053.
11 (*a*) T. V. Jones, R. A. Blatchly and G. N. Tew, *Org. Lett.*, 2003, **5**, 3297; (*b*) T. V. Jones, M. M. Slutsky, R. Laos, T. F. A. de Greef and G. N. Tew, *J. Am. Chem. Soc.*, 2005, **127**, 17235; (*c*) M. M. Slutsky, T. V. Jones and G. N. Tew, *J. Org. Chem.*, 2007, **72**, 342.
12 C. R. Ray and J. S. Moore, *Adv. Polym. Sci.*, 2005, **177**, 91.
13 L. Brunsveld, R. B. Prince, E. W. Meijer and J. S. Moore, *Org. Lett.*, 2000, **2**, 1525.
14 (*a*) B. M. W. Langeveld-Voss, R. A. Janssen, M. P. T. Christiaan, S. C. J. Meskers, H. P. J. M. Dekkers and E. W. Meijer, *J. Am. Chem. Soc.*, 1996, **118**, 4908; (*b*) A. P. H. J. Schenning, P. Jonkheijm, E. Peeters and E. W. Meijer, *J. Am. Chem. Soc.*, 2001, **123**, 409.
15 (*a*) V. Berl, I. Huc, R. G. Khoury and J. M. Lehn, *Chem.–Eur. J*, 2001, **7**, 2810; (*b*) V. Berl, I. Huc, R. G. Khoury, M. J. Krische and J. M. Lehn, *Nature*, 2000, **407**, 720.
16 C. Dolain, C. L. Zhang, M. J. Leger, L. Daniels and I. Huc, *J. Am. Chem. Soc.*, 2005, **127**, 2400.
17 Individual proton resolution is lost here, so it could be possible that one or more protons shifts downfield although the major changes between the two spectra involve upfield shifts.
18 (*a*) R. B. Prince, J. S. Moore, L. Brunsveld and E. W. Meijer, *Chem.–Eur. J.*, 2001, **7**, 4150; (*b*) R. B. Prince, L. Brunsveld, E. W. Meijer and J. S. Moore, *Angew. Chem., Int. Ed.*, 2000, **39**, 228.
19 D. Seebach and J. L. Matthews, *Chem. Commun.*, 1997, 2015.
20 A. F. M. Kilbinger, A. P. H. J. Schenning, F. Goldoni, W. J. Fease and E. W. Meijer, *J. Am. Chem. Soc.*, 2000, **122**, 1820.
21 M. Inouye, M. Waki and H. Abe, *J. Am. Chem. Soc.*, 2004, **126**, 2022.

22 R. B. Prince, S. A. Barbes and J. S. Moore, *J. Am. Chem. Soc.*, 2000, **122**, 2758.
23 L. Brunsveld, E. W. Meijer, R. B. Prince and J. S. Moore, *J. Am. Chem. Soc.*, 2001, **123**, 7978.
24 S. H. Seo, T. V. Jones, H. Seyler, J. O. Peters, T. H. Kim, J. Y. Chang and G. N. Tew, *J. Am. Chem. Soc.*, 2006, **128**, 9264.
25 (*a*) P. Talukdar, G. Bollot, J. Mareda, N. Sakai and S. Matile, *Chem.–Eur. J.*, 2005, **11**, 6525; (*b*) N. Sakai, P. Talukdar and S. Matile, *Chirality*, 2006, **18**, 91; (*c*) M. Wolffs, S. J. George, Z. Tomovic, S. C. J. Meskers, A. P. H. J. Schenning and E. W. Meijer, *Angew. Chem., Int. Ed.*, 2007, **46**, 8203; (*d*) B. M. W. Langeveld-Voss, R. A. J. Janssen and E. W. Meijer, *J. Mol. Struct.*, 2000, **521**, 285; (*e*) K. Nakanishi and N. Berova, The Exciton Chirality Method, in *Circular Dichroism—Principles and Applications*, ed. K. Nakanishi, N. Beroca and R. W. Woody, VCH, Weinheim, Germany, 1994, pp. 361–398.

